Dissecting Xuesaitong's mechanism on preventing stoke based on microarray and connectivity map

Journal:	*Molecular BioSystems*
Manuscript ID:	MB-ART-06-2015-000379.R1
Article Type:	Paper
Date Submitted by the Author:	07-Aug-2015

Complete List of Authors:	Wang, Linli; Pharmaceutical Informatics Institute, College of Pharmaceutical Sciences, Zhejiang University Yu, Yunru; Pharmaceutical Informatics Institute, College of Pharmaceutical Sciences, Zhejiang University Yang, Jihong; Pharmaceutical Informatics Institute, College of Pharmaceutical Sciences, Zhejiang University Zhao, Xiaoping; Zhejiang Chinese Medical Universit, College of Preclinical Medicine Li, Zheng; Tianjin University of Traditional Chinese Medicine, State Key Laboratory of Modern Chinese Medicine

Dissecting Xuesaitong's mechanism on preventing stoke based on microarray and connectivity map

Linli Wang[1], Yunru Yu[1], Jihong Yang[1], Xiaoping Zhao[2, *], Zheng Li[3, *]

[1]*Pharmaceutical Informatics Institute, College of Pharmaceutical Sciences, Zhejiang University, Hangzhou 310058, China; n 300193, China;*

[2]*College of Preclinical Medicine, Zhejiang Chinese Medical University, Hangzhou 310053, China;*

[3]*State Key Laboratory of Modern Chinese Medicine, Tianjin University of Traditional Chinese Medicine, Tianjin, China.*

[*]*Correspondence should be addressed to Dr. Zheng Li (lizheng1@gmail.com), phone: +86-571-88208427 or Dr. Xiaoping Zhao (zhaoxiaoping@zjtcm.net), phone: +86-571-86633138.*

Graph abstract

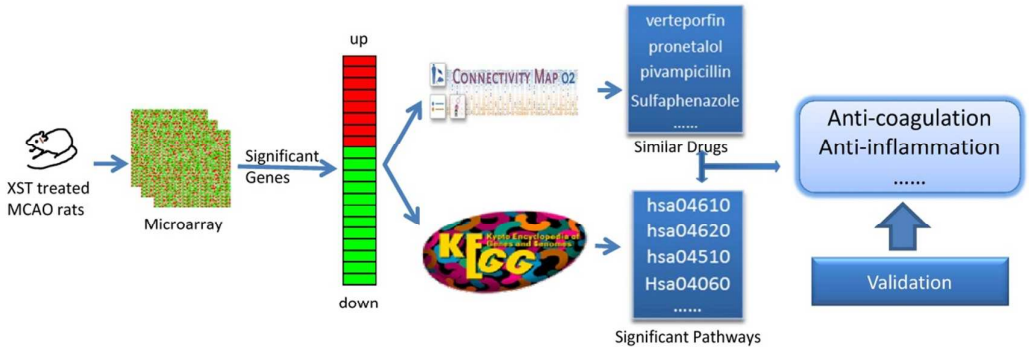

Dissecting the mode of action of Xuesaitong injection on preventing cerebral ischemia-reperfusion injury based on the combination of gene expression data analysis and connectivity map

Abstract

Elucidating action mechanisms of Chinese medicines has remained a challenging task due to the chemical and biological complexity that needs to be resolved. In this study we applied a gene expression data and Connectivity Map (CMAP) based approach to study action mechanisms of a Chinese medicine Xuesaitong injection (XST) on preventing cerebral ischemia-reperfusion injury. XST is a standardized patent Chinese medicine of *Panax notoginseng* roots and it has long been used for effective prevention and treatment of stroke in China. However, more research is needed to understand the mechanisms underlying its effects against ischemic stroke. We first evaluated the effect of XST against ischemic stroke in an ischemia-reperfusion rat animal model and dissected its mechanisms based on gene expression data of injured brain. The results showed that treatment with XST significantly attenuated infarct area and histological damage. Based upon pathway analysis and CMAP query of microarray data, anti-inflammatory response and anti-platelet coagulation were found as the major mechanisms of XST against stroke, which were further validated *in vitro* and with pharmacological assays of serum. We demonstrated the feasibility of applying the combination of microarray with CMAP in identifying mechanisms of Chinese medicine.

Introduction

Chinese medicine has been developed through thousands of years of empirical applications in China. It has made remarkable contributions to promoting the health and longevity of human welfare[1, 2]. The clinical efficacy of Chinese medicine in various pathological conditions has been widely recognized and reported. However, the mechanisms of many Chinese medicines remain elusive, despite of enormous research efforts carried out in recent decades[3]. One of the major reasons is that Chinese medicine is a multiple component system and it treats diseases with multiple targets, multiple pathways and multiple actions[4]. The vast chemical and biological complexity of the action mechanisms needs to be revealed with systematic approaches.

Panax notoginseng (Burk.) FH Chen is one of the most widely used herbal medicines for cardio-cerebral vascular diseases in China[5-8]. Xuesaitong injection (XST) is a prescription drug made of *Panax notoginseng* and Panax notoginseng saponins (PNS) are its main active components[9]. Ginsenoside Rg1, Rb1, Re and Rd and notoginsenoside R1 were found to account for ~85% of the total compositions in XST in our previous study[10]. The major components are well quantified, controlled and subjected to standardization[10]. The effective clinical treatment of acute ischemia stroke by XST has been reported[11, 12], although some reports may be limited by small sample sizes[5, 13]. Potential mechanisms include attenuating the apoptosis, modulating inflammatory response of microglia[14-16], but a systematic study on the mechanisms of XST is still missing.

The development of transcriptional omics approach provides an opportunity to simultaneously analyze a large number of genes associated with disease and complex therapeutic effects of medicines, e.g. Chinese medicine[4, 17, 18]. The analysis of genes modulated by Chinese medicine may provide insights into its molecular mechanisms. Connectivity Map (CMAP), a similarity-based method, is one of the most effective tools for mode-of-action study. CMAP is a systematic approach developed for the discovery of functional connections among diseases, genes and drugs through the genome-wide transcriptional expression data and the transitory feature of common gene-expression changes[19]. CMAP contains more than 7,000 expression profiles representing 1,309 compounds. Drugs affecting common gene expressions can be identified through CMAP analysis, which provides a useful tool for discovering the mode of action of drugs, such as Chinese medicine[20-23]. For example, Zhi ning *et al*[22] applied the combined microarray and CMAP approach in identifying molecular mechanisms of Si-Wu-Tang.

To evaluate the effect and mechanisms of XST on preventing stroke, a rat animal model was produced with middle cerebral artery occlusion (MCAO) procedure and treated with XST for seven days. In this study, XST's effects on infarction area and histological damage in MCAO rats were studied firstly. Then, the gene expression profile in injured brains was also measured. A combined approach of pathway and CMAP analysis was further used to identify molecular mechanisms of XST. As a result, anti-inflammation and anti-platelet coagulation were identified as the major mechanisms of XST against ischemic stroke. We demonstrated an approach in

identifying molecular mechanisms of Chinese medicine by combining microarray data and CMAP approach.

Materials and Methods

Animals

Adult male Sprague-Dawley rats were purchased from Weitong-Lihua Experimental Animal Co. Ltd. (Beijing, China). All animal procedures were approved by the Institutional Animal Care and Use Committee (IACUC, China) and the experimental animal protocols were approved by the Institutional Animal Ethical Committee of Tianjin Centre for Drug Safety Assessment (Tianjin, China).

Drug and reagents

XST lyophilized powder for injection, one of the major types of XST Injection used in clinical practices was manufactured by Heilongjiang Zhenbaodao pharmaceutical Co. Ltd. (Heilongjiang, China). It was dissolved in saline before experiment. 2, 3, 5-Triphenyltetrazolium chloride (TTC) was purchased from Beijing Solarbio Science & Technology Co., Ltd. Rat thromboxane B_2 (TXB_2), 6-keto $PGF_{1\alpha}$ enzyme linked immunosorbent assay (ELISA) Kits were from Bio-Swamp.

Experimental protocol

Rats were subjected to MCAO and reperfusion[24, 25]. Briefly, animals were anesthetized with isoflurane, neck vessels were exposed and branches of the right external carotid artery were isolated. The right middle cerebral artery was occluded with a 0.25 mm nylon monofilament by inserting it through right external carotid artery to produce the cerebral focal ischemia. Two hours after occlusion, the inserted

filament was slowly withdrawn to allow reperfusion. The incision on the neck was closed. Fifteen Sham-operated rats underwent the same surgical procedures but without the insertion of the nylon filament into the inner carotid. Successful MCAO rats were randomly divided into four groups (with fifteen rats in each group). Three dose of XST were given to rats: 20 mg/kg, 40 mg/kg and 80 mg/kg for low (XSTL), medium (XSTM), and high (XSTH) concentrations, respectively. Sham and Model groups received equivalent vehicle. All the treatments were given once daily with intravenous injection consecutively for seven days.

Infarct area measurement and Brain histology

At the end of the experiment, rats were anesthetized with chloral hydrate (360 mg/kg), arterial blood samples were collected at aorta abdominalis. Rat brains were quickly removed. Ten rat brains in each group were frozen at −20°C and sectioned into 2 mm-thick coronal slices. Slices were incubated for 10 min at 37 °C in 2% TTC solution in phosphate buffered saline (PBS, pH 7.4). And in each sample, the infarction area ratio was calculated by dividing the total infarction area by the total slice area.

The infarcted hemispheres of remaining five rat brains in each group were divided into two parts: one for histological test, and one for microarray experiment. The hemispheres for histological test were fixed in 10% formaldehyde solution, and embedded in paraffin. The paraffin sections (5μm) were stained with hematoxylin and eosin (HE) and analyzed by light microscopy.

Microarray experiment and data analysis

We profiled the gene expressions in the infarcted hemispheres of Sham, Model and XSTH groups (n=5) using Affymetrix Rat 230 2.0 Array. The detailed procedure of microarray experiment was the same as described previously[4]. The dataset as CEL files was deposited to GEO and the access number is GSE61616. Global scaling normalization of the expression data was performed with Median Scaling Normalization in ArrayTrack 3.5.0[26] using a target median value of 1000. Genes associated with stroke were obtained from databases including SIDD, DISEASES, DisGeNet, MALACARDS, DGA with keywords 'Brain infarction', 'Ischemic stroke', 'Stroke', 'Stroke, Ischemic', 'Brain Ischemia', or "Cerebrovascular Accident". The fold change (FC) of stroke related genes between Model and Sham (as FC1) were calculated, as well as between Model and XSTH (as FC2). The Reverse Rate (RR) was also calculated as previously reported[4] and genes with RR >0 mean they were positively regulated by XST. Genes with FC1>1.5, FC2>1.2 and RR >0 were defined as differentially expressed genes by XST. The list of differentially expressed genes was imported to the Kyoto Encyclopedia of Genes and Genomes (KEGG) database through ArrayTrack 3.5.0 for functional enrichment analysis.

To better understand the mechanisms of XST, the similarities of the gene expression profile between XST and chemical drugs were measured through the CMAP (http://www.broadinstitute.org/cMAP/) reference database (Build 02). The differentially expressed genes were divided into two parts, one for up-regulation and the other for down-regulation by XST. In order to query the CMAP, the genes were converted to probe sets in chip type Affymetrix GeneChip Human Genome HT

U133A Array. Then they were used as queries to search the CMAP. The similarity between XST and a CMAP instance is measured by an enrichment score, ranging from -1 to 1 and a permutation p-value. Chemicals with p-value<0.05 and positive enrichment score were defined as significantly related.

Real-time reverse-transcription polymerase chain reaction

The transcripts for six representative different genes were quantified by real-time reverse-transcription polymerase chain reaction (RT-PCR). Total RNA was obtained from the microarray experiment. Template RNA was reverse transcribed to cDNA using QuantiTect Reverse Transcription Kit (Qiagen) according to the manufacturer's instructions. The relative expressions of mRNAs were detected using QuantiFast SYBR Green PCR Kit (Qiagen). In order to normalize variations in mRNA extraction and cDNA synthesis, the expression of beta-actin (Actb) was measured simultaneously. All primer sets were purchased from Takara (Dalian, China) and Beijing Genomics Institute (BGI, Shenzhen, China). Triplicate aliquot reactions were carried out for each sample at 95°C for 5 minutes followed by 40 cycles of denaturation at 95°C for 10 seconds and combined annealing/extension at 60°C for 30 seconds. Data were quantified using the 2-delta CT method[27, 28]. Primers used for real-time PCR were shown in Table 1.

Measurement of platelet aggregation and TXB_2 and 6-keto $PGF_{1\alpha}$

Arterial blood samples were collected and anti-coagulated with 3.2% of sodium citrate (ratio 9:1). Platelet-rich plasma (PRP), obtained by centrifuging whole blood

for 10 minutes at 800 rpm, was stimulated with ADP of final concentration about 4 μmol/L. Platelet aggregation was monitored by light transmission in Chrono-log 540 aggregometer (Chrono-log Corp., Haverton, PA, USA) with continuous stirring at 37°C. The 100% line was set using platelet-poor plasma (PPP) and the 0 baseline established with PRP (adjusted from 3.5×10^8 platelets/ml up to 4×10^8 platelets/ml). PPP was prepared by centrifuging whole blood for 10 minutes at 3000 rpm. TXB_2 and 6-keto $PGF_{1\alpha}$ levels were measured according to manufacturer instructions

in vitro validation of anti-inflammation action of XST

RAW264.7 cells were obtained from the Cell Bank of Type Culture Collection of the Chinese Academy of Sciences (Shanghai, China) and cultured at 37°C in 5% CO2 in DMEM containing 10% heat-inactivated FBS. The RAW264.7 cells were plated at a density of 3×10^4 per well in a 96-well plate. Twenty-four hours later, cells were pre-treated with indicated concentrations of XST (2.5, 5, 10, 25, 50, 100 and 200 μ g/ml) or indomethacin (Indo, 25 μ M) for another 6 h, followed by treatment with LPS (50 ng/ml) for an additional 24 h. Indo was a positive control. The amount of NO production in the medium was detected with the Griess reaction (Beyotime Institute of Biotechnology, China). The absorbance of the mixture at 550 nm was determined with a microplate reader, and nitrite concentration was determined using a dilution of sodium nitrite as a standard.

Statistical Analysis

All values are given as mean ± standard deviation. Statistical analysis was performed using SPSS software. One-way analysis of variance (ANOVA) was used to compare

group variables, comparisons of parameters between two groups were performed with least significant differences (LSD) or Games-Howell test[29, 30]. Differences were considered significant if p-value was less than 0.05.

Results

XST reduced infarct size in brains

No infarct area was observed in the Sham group. In contrast, noticeable infarct areas were observed in Model group as evidenced by a large TTC-negatively-stained area in cortex and striatum. As compared to Model group, intravenous administration of XST protected rat brains against MCAO injury to a significant degree (As shown in Figure.1). XST at 40, and 80 mg/kg significantly reduced the infarct size by 25.2% ($p < 0.05$) and 26.9% ($p < 0.05$) in comparison to the Model group.

Effect of XST on cortex histology in MCAO rats

Figure.2 showed the results of histological examination of the cortex of right brain in different groups. Compared with Sham group, distinct alterations occurred in MCAO rats, including abundant eosinophilic cytoplasm, karyopyknosis, swelling and damage of neurons, cavitation of cytoplasm. All of these alterations were ameliorated by treatment with XST, especially in XSTH group.

Microarray data analysis

1205 stroke related genes were obtained from five databases. However, only 212 genes were identified as XST significantly regulated genes against stroke in our setting . Detailed gene lists were provided in Table S1.

To gain deeper biological insights, the genes were further categorized into functional

pathways in KEGG database. There were 24 KEGG pathways significantly enriched with fisher P value less than 0.05. The top 15 significantly impacted KEGG pathways were listed in Table 2. Among them, Cytokine-cytokine receptor interaction has the largest number of enrichment genes and minimal Fisher P value. Cytokine-cytokine receptor interaction, Focal adhesion and ECM-receptor interaction were correlated with adhesion. Four pathways: Complement and coagulation cascades, Toll-like receptor signaling pathway, Leukocyte transendothelial migration, and Intestinal immune network for IgA production were classified to Immune System/Cellular Processes, which were involved in immune responses, inflammatory response and coagulation. Arachidonic acid metabolism is closely related to the production of inflammatory factors and blood coagulation factors. MAPK signaling pathway and p53 signaling pathway have important functions proliferation and apoptosis. In summary, inflammatory immune response, coagulation and apoptosis were the major mechanisms of XST against stroke based on pathway analysis.

Mapping gene expression profiles to CMAP

The significantly regulated genes by XST were converted to 67 up-regulated and 300 down-regulated probe sets, and they were used as the query to the CMAP. Eighteen drugs with p-value<0.05 and positive enrichment score were found by CMAP (Table 3). Among them, non-steroidal anti-inflammatory drug glafenine and parthenolide[31] are anti-inflammatory agents. Piperlongumine has anti-plate aggregation effect[32]. Pivampicillin, sulfaphenazole, sulfathiazole, nifuroxazide, parthenolide[33] and caffeic acid[34] were all antibacterials. Papaverine and difenidol could dilate blood vessel. β

-blocker pronetalol and cardiac glycoside ouabain are involved in the regulation of heart muscle function.

Real-time RT-PCR validation of selected genes

To validate the findings from microarray data set, the expression levels of six representative genes were confirmed with RT-PCR. We found that Fabp4, Plau, Ltc4s, Igf1, Spp1, Timp1 and Hmox1 were highly up-regulated by MCAO, and suppressed by XST treatment, which showed similar patterns with microarray data. The FCs in microarray and RT-PCR were listed in Table 4.

XST decreased platelet aggregation and ameliorated the changes of TXB_2 and 6-keto $PGF_{1\alpha}$

XST significantly decreased platelet aggregation in a dose-dependent manner as compared with Model group (Figure.3). XST at 20, 40, and 80 mg/kg reduced the maximum platelet aggregation rate by 10.2%, 18.2% and 22.8%. After MCAO, the serum level of TXB_2 increased significantly as compared with sham-operated rats ($P< 0.05$) and 6-keto $PGF_{1\alpha}$ decreased. XST (20, 40, and 80 mg/kg) ameliorated these changes in a dose-dependent manner (Figure.4).

in vitro validation of anti-inflammation action of XST

To evaluate the inhibitory effect of XST on LPS-mediated production of inflammatory cytokines, the amount of NO production was determined by the amount of nitrite, a stable metabolite of NO. As shown in Figure.5, RAW264.7 macrophages produced 0.35 ± 0.11 μM nitrite in the resting state. After LPS stimulation for 24h, NO production increased to 6.98 ± 0.50 μM. XST inhibited the nitrite production in a

dose-dependent manner. 200 μg/ml of XST could suppresses the NO production stimulated by LPS completely. XST can inhibit NO production significantly at 50 μg/ml.

Discussion

Stroke is the second leading cause of death in China and worldwide with high morbidity, disability and death rates[35, 36]. Ischemic stroke accounted for almost eighty five percent of all strokes[37]. Tissue plasminogen activator is the only approved therapy for ischemic stroke treatment[38, 39]. But less than 10% of patients received this therapy because of its narrow therapeutic time window and the risk of intracranial hemorrhagic transformation[40-43]. Therefore, discovering safe and effective drugs and treatment approach for stroke to restore neural function and reduce disabilities with a wide therapeutic window is an important but daunting task[44]. Chinese medicine would be an important resource for stroke treatment and new drug development. Among them, an attractive one is *Panax notoginseng* (Burk.) FH Chen[9, 45]. Its product XST has been extensively used for the treatment and prevention of stroke in China.

Panax notoginseng belongs to "HuoXueHuaYu" medicines in traditional Chinese medicine, which means "blood-activating and stasis-dissolving". In this study, coagulation related pathways and anti-plate aggregation drugs were significantly enriched by high dose of XST through pathway enrichment and CMAP analysis. Moreover, the inhibition of anti-plate aggregation effect was also validated in serum test. Thrombosis is the most common trigger and a subsequent injury factor and it plays a key role in the occurrence of ischemic stroke. Therefore anti-plate aggregation

is one of the important mechanisms for XST in stroke treatment, ginsenoside Rg1 could be one of the effective ingredient[46, 47].

Inflammation is an essential process in ischemic stroke pathology. Activated macrophages induce severe inflammation which causes cerebral swelling[48]. In this study, inflammation and adhesion is another important mechanism of XST against stroke. The class of inflammation-related pathways was the largest in all pathways enriched by significant genes. Two anti-inflammatory drugs were significantly identified in CMAP analysis. We further validated the anti-inflammatory action *in vitro*, as XST inhibited inflammatory factor in RAW 264.7 cells in a dose-dependent manner, and high dose of XST could prevent NO production completely. The results confirmed the anti-inflammatory effect of XST. Several reports[49-51] revealed that ginsenoside Rd might be involved in anti-inflammatory effect in neuroprotection after focal cerebral ischemia, and it would be one of the effective ingredients.

Interestingly, CMAP analysis also identified several anti-infection drugs being similar to XST, which needs further studies to validate the anti-infection effect of XST and its contribution to stroke treatment. A meta-analysis in 2013 demonstrated that 30% of acute stroke patients complicated in infection[52]. Anti-infection is a very important aspect in stroke treatment.

In conclusion, the present study demonstrated an effective approach in identifying molecular mechanisms of XST against stroke by combining the use of disease-specific microarray with CMAP analysis. First, we demonstrated that XST was able to attenuate ischemia-reperfusion induced brain injury. After an integrated

analysis of the microarray data and CMAP query, inhibition of inflammatory response and coagulation were identified as the major mechanisms involved in the protective effects of XST.

Conflict of Interests

The authors claim no conflict of interests.

Acknowledgements

This work was financially supported by the National Natural Science Foundation of China (No. 81273991). The rat experiment was carried out in Tianjin Institute of Pharmaceutical Research by Prof. Zhuanyou Zhao's lab. And Microarray test was performed in Shanghai Biotechnology Corporation.

Reference

1. Y. Tu, *Nature medicine*, 2011, **17**, 1217-1220.
2. F. Cheung, *Nature*, 2011, **480**, S82-S83.
3. X. Wang, A. Zhang and H. Sun, *Omics: a journal of integrative biology*, 2012, **16**, 414-421.
4. L. Wang, Z. Li, X. Zhao, W. Liu, Y. Liu, J. Yang, X. Li, X. Fan and Y. Cheng, *Evidence-Based Complementary and Alternative Medicine*, 2013, **2013**.
5. X. Chen, M. Zhou, Q. Li, J. Yang, Y. Zhang, D. Zhang, S. Kong, D. Zhou and L. He, *Stroke*, 2009, **40**, e394-e395.
6. T. Ng, *Journal of pharmacy and pharmacology*, 2006, **58**, 1007-1019.
7. Q. Shang, H. Xu, Z. Liu, K. Chen and J. Liu, *Evidence-Based Complementary and Alternative Medicine*, 2013, **2013**.
8. X. Yang, X. Xiong, H. Wang and J. Wang, *Evidence-based complementary and alternative medicine : eCAM*, 2014, **2014**, 204840.
9. X. Chen, M. Zhou, Q. Li, J. Yang, Y. Zhang, D. Zhang, S. Kong, D. Zhou and L. He, *Cochrane Database Syst Rev*, 2008, **4**.
10. L. Wang, Z. Li, Q. Shao, X. Li, N. Ai, X. Zhao and X. Fan, *Molecular bioSystems*, 2014, **10**, 1905-1911.

11. L. He, X. Chen, M. Zhou, D. Zhang, J. Yang, M. Yang and D. Zhou, *Phytomedicine*, 2011, **18**, 437-442.
12. Z. Shang-qian, S. Li-jing, Y. Yu-zhen, S. Yan-qin and Z. Yin-yuan, *Chinese journal of integrative medicine*, 2005, **11**, 128-131.
13. X. M. Zhang, J. R. Wu and B. Zhang, *Bmc Complem Altern M*, 2015, **15**.
14. H. Li, C.-Q. Deng, B.-Y. Chen, S.-P. Zhang, Y. Liang and X.-G. Luo, *Journal of ethnopharmacology*, 2009, **121**, 412-418.
15. L. Liu, L. Zhu, Y. Zou, W. Liu, X. Zhang, X. Wei, B. Hu and J. Chen, *Biological & pharmaceutical bulletin*, 2014.
16. H. Y. Son, H. S. Han, H. W. Jung and Y.-K. Park, *Journal of pharmacological sciences*, 2009, **109**, 368-379.
17. Z. Fang, B. Lu, M. Liu, M. Zhang, Z. Yi, C. Wen and T. Shi, *PLoS One*, 2013, **8**, e72334.
18. A. Buriani, M. L. Garcia-Bermejo, E. Bosisio, Q. Xu, H. Li, X. Dong, M. S. Simmonds, M. Carrara, N. Tejedor and J. Lucio-Cazana, *Journal of ethnopharmacology*, 2012, **140**, 535-544.
19. J. Lamb, E. D. Crawford, D. Peck, J. W. Modell, I. C. Blat, M. J. Wrobel, J. Lerner, J. P. Brunet, A. Subramanian, K. N. Ross, M. Reich, H. Hieronymus, G. Wei, S. A. Armstrong, S. J. Haggarty, P. A. Clemons, R. Wei, S. A. Carr, E. S. Lander and T. R. Golub, *Science*, 2006, **313**, 1929-1935.
20. G. Wei, D. Twomey, J. Lamb, K. Schlis, J. Agarwal, R. W. Stam, J. T. Opferman, S. E. Sallan, M. L. den Boer and R. Pieters, *Cancer cell*, 2006, **10**, 331-342.
21. H. Hieronymus, J. Lamb, K. N. Ross, X. P. Peng, C. Clement, A. Rodina, M. Nieto, J. Du, K. Stegmaier and S. M. Raj, *Cancer cell*, 2006, **10**, 321-330.
22. Z. Wen, Z. Wang, S. Wang, R. Ravula, L. Yang, J. Xu, C. Wang, Z. Zuo, M. S. Chow, L. Shi and Y. Huang, *PLoS One*, 2011, **6**, e18278.
23. A. C. Ravindranath, N. Perualila-Tan, A. Kasim, G. Drakakis, S. Liggi, S. C. Brewerton, D. Mason, M. J. Bodkin, D. A. Evans, A. Bhagwat, W. Talloen, H. W. Gohlmann, Z. Shkedy, A. Bender and Q. Consortium, *Molecular bioSystems*, 2015, **11**, 86-96.
24. P. Wang, T. Y. Xu, Y. F. Guan, W. W. Tian, B. Viollet, Y. C. Rui, Q. W. Zhai, D. F. Su and C. Y. Miao, *Annals of neurology*, 2011, **69**, 360-374.
25. J. Li, R.-g. Wu, F.-y. Meng, Z. Wang, C.-m. Wang, Y.-y. Wang and Z.-j. Zhang, *PloS one*, 2012, **7**, e45811.
26. W. Tong, X. Cao, S. Harris, H. Sun, H. Fang, J. Fuscoe, A. Harris, H. Hong, Q. Xie and R. Perkins, *Environmental health perspectives*, 2003, **111**, 1819.
27. D.-H. Yang, K. K. McKee, Z.-L. Chen, G. Mernaugh, S. Strickland, R. Zent and P. D. Yurchenco, *Development*, 2011, **138**, 4535-4544.
28. S. Nagel, G. Hadley, K. Pfleger, C. Grond‐Ginsbach, A. M. Buchan, S. Wagner and M. Papadakis, *Journal of neurochemistry*, 2012, **123**, 98-107.
29. T. Ma, H. Liu, W. Chen, X. Xia, X. Bai, L. Liang, Y. Zhang and T. Liang, *American Journal of Transplantation*, 2012, **12**, 620-629.
30. Z. Djuric, M. Kashif, T. Fleming, S. Muhammad, D. Piel, R. von Bauer, F. Bea, S. Herzig, M. Zeier, M. Pizzi, B. Isermann, M. Hecker, M. Schwaninger, A. Bierhaus and P. P. Nawroth, *Molecular medicine*, 2012, **18**, 1375-1386.
31. S. Li, X. Gao, X. Wu, Z. Wu, L. Cheng, L. Zhu, D. Shen and X. Tong, *Acta biochimica et biophysica Sinica*, 2015, **47**, 368-375.
32. M. Iwashita, N. Oka, S. Ohkubo, M. Saito and N. Nakahata, *European journal of pharmacology*,

2007, **570**, 38-42.

33. T. Onozato, C. V. Nakamura, D. A. Cortez, B. P. Dias Filho and T. Ueda-Nakamura, *Phytotherapy research : PTR*, 2009, **23**, 791-796.
34. S. Perumal, R. Mahmud and S. Ramanathan, *Natural product research*, 2015, DOI: 10.1080/14786419.2014.999242, 1-4.
35. V. L. Feigin, M. H. Forouzanfar, R. Krishnamurthi, G. A. Mensah, M. Connor, D. A. Bennett, A. E. Moran, R. L. Sacco, L. Anderson and T. Truelsen, *The Lancet*, 2013.
36. Q. Wang, C. Gao, H. Wang, L. Lang, T. Yue and H. Lin, *PloS one*, 2013, **8**, e80381.
37. J. R. Kizer and R. B. Devereux, *New England Journal of Medicine*, 2005, **353**, 2361-2372.
38. J. R. Marler, T. Brott, J. Broderick, R. Kothari, M. Odonoghue, W. Barsan, T. Tomsick, J. Spilker, R. Miller and L. Sauerbeck, *New England Journal of Medicine*, 1995, **333**, 1581-1587.
39. J. L. Saver, G. C. Fonarow, E. E. Smith, M. J. Reeves, M. V. Grau-Sepulveda, W. Pan, D. M. Olson, A. F. Hernandez, E. D. Peterson and L. H. Schwamm, *JAMA*, 2013, **309**, 2480-2488.
40. D. Kleindorfer, C. J. Lindsell, L. Brass, W. Koroshetz and J. P. Broderick, *Stroke*, 2008, **39**, 924-928.
41. M. Reeves, S. Arora, J. Broderick, M. Frankel, J. Heinrich, S. Hickenbottom, H. Karp, K. LaBresh, A. Malarcher and G. Mensah, *Stroke*, 2005, **36**, 1232-1240.
42. A. K. Boehme, R. B. Shahripour, J. T. Houston, P. V. Rawal, N. Kapoor and A. V. Alexandrov, 2013.
43. M. J. Lyerly, K. C. Albright, A. K. Boehme, R. Bavarsad Shahripour, J. T. Houston, P. V. Rawal, N. Kapoor, M. Alvi, A. Sisson and A. W. Alexandrov, *Journal of Stroke and Cerebrovascular Diseases*, 2014, **23**, 855-860.
44. A. Shehadah, J. Chen, B. Kramer, A. Zacharek, Y. Cui, C. Roberts, M. Lu and M. Chopp, *PloS one*, 2013, **8**, e54083.
45. B. Wu, M. Liu, H. Liu, W. Li, S. Tan, S. Zhang and Y. Fang, *Stroke*, 2007, **38**, 1973-1979.
46. Q. Zhou, L. Jiang, C. Xu, D. Luo, C. Zeng, P. Liu, M. Yue, Y. Liu, X. Hu and H. Hu, *Thrombosis Research*, 2014, **133**, 57-65.
47. H. L. Xu, Y. Ji and M. R. Rao, *Chinese Journal of Pharmacology and Toxicology*, 1998, **12**, 40-42.
48. T. Shichita, M. Ito and A. Yoshimura, *Frontiers in cellular neuroscience*, 2014, **8**, 319.
49. R. Ye, Q. Yang, X. Kong, J. Han, X. Zhang, Y. Zhang, P. Li, J. Liu, M. Shi, L. Xiong and G. Zhao, *Neurochemistry International*, 2011, **58**, 391-398.
50. R. Ye, X. Kong, Q. Yang, Y. Zhang, J. Han and G. Zhao, *Neuropharmacology*, 2011, **61**, 815-824.
51. G. Hu, Z. Wu, F. Yang, H. Zhao, X. Liu, Y. Deng, M. Shi and G. Zhao, *Neurological Sciences*, 2013, **34**, 2101-2106.
52. W. F. Westendorp, P. J. Nederkoorn, J. D. Vermeij, M. G. Dijkgraaf and D. van de Beek, *BMC neurology*, 2011, **11**, 110.

Figure legend

Figure 1. The effect of XST on infarct size in rat brains. The infarction area ratio was calculated by dividing the total infarction area by the total slice area. Values are means ± SD (n = 10 for each). *P < 0.05 *vs.* Model group.

Figure 2. The effect of XST on brain histology. Histology (H.E., haematoxylin and Eosin) of the rat brains from Sham group (A), Model group (B), XSTL group (C), XSTM group (D), and XSTH group (E). Abundant eosinophilic cytoplasm, karyopyknosis, swelling and damage of neurons, cavitation of cytoplasm were ameliorated by XST treatment.

Figure 3. The effect of XST on the maximum platelet aggregation rate. The maximum platelet aggregation rates of rats in different groups were measured. Values are means ± SD (n = 15 for each). *P < 0.05*vs.* Model group.

Figure 4. The effect of XST on TXB_2 and 6-keto $PGF_{1\alpha}$ in sera (n = 15). TXB2 and 6-keto PGF1α levels in sera in different groups were measured. Presented are the changes of TXB_2 (A), 6-keto $PGF_{1\alpha}$ (B). Values are means ± SD. $^{\#}P < 0.05$ and $^{\#\#}P < 0.01$ *vs.* Sham group; *P < 0.05 and ***P < 0.001 *vs.* Model group.

Figure 5. The effect of XST on NO production in RAW264.7 macrophages. Cells were treated simultaneously with 50 ng/ml LPS and 2.5~200 μg/ml of XST. Supernatants were collected after 24 h and assayed for NO. Values are means ± SD. $^{\#\#}P < 0.01$*vs.* Control; *P < 0.05 and **P < 0.01*vs.* LPS-stimulated cells.

Figure 1. The effect of XST on infarct size in rat brains.

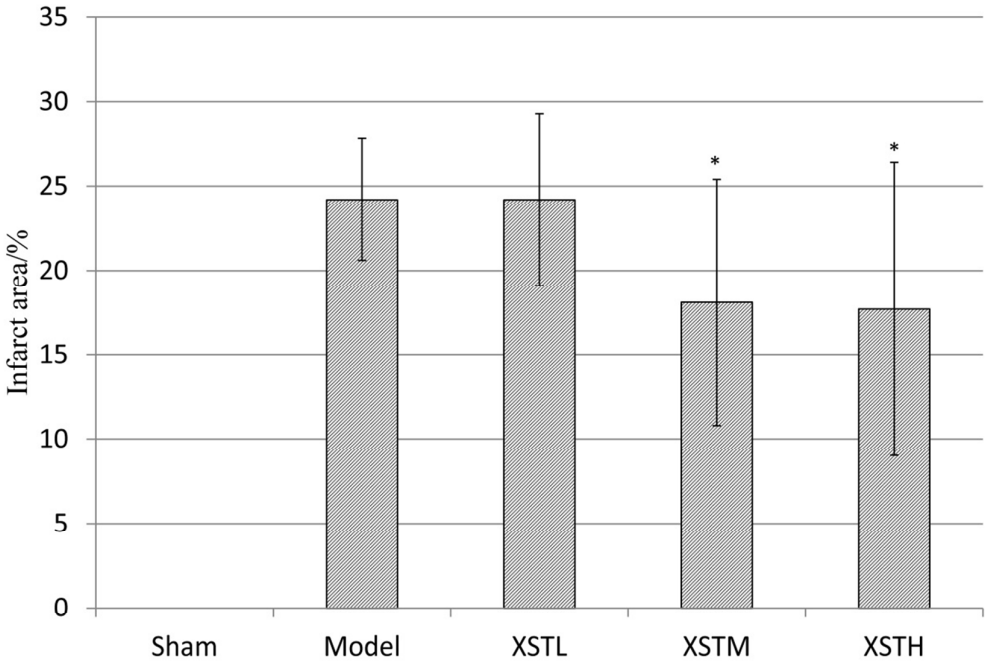

Figure 2. The effect of XST on brain histology.

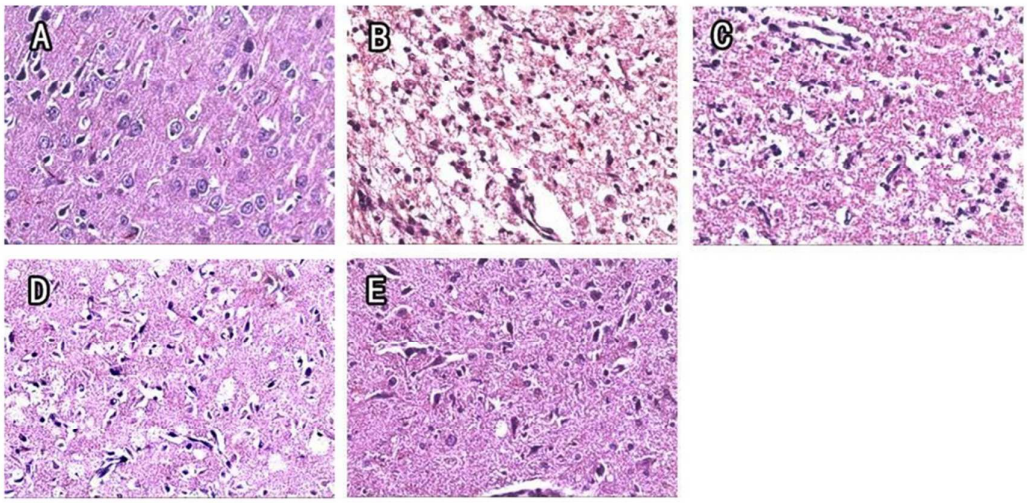

Figure 3. The effect of XST on the maximum platelet aggregation rate.

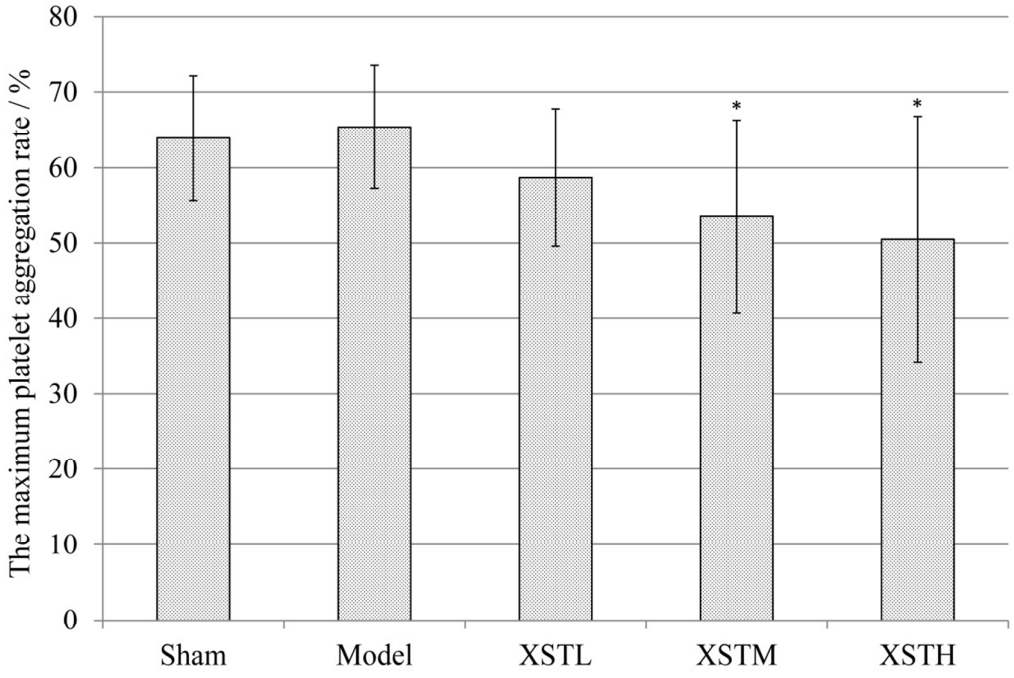

Figure 4. The effect of XST on TXB_2 and 6-keto $PGF_{1\alpha}$ in sera (n = 15)

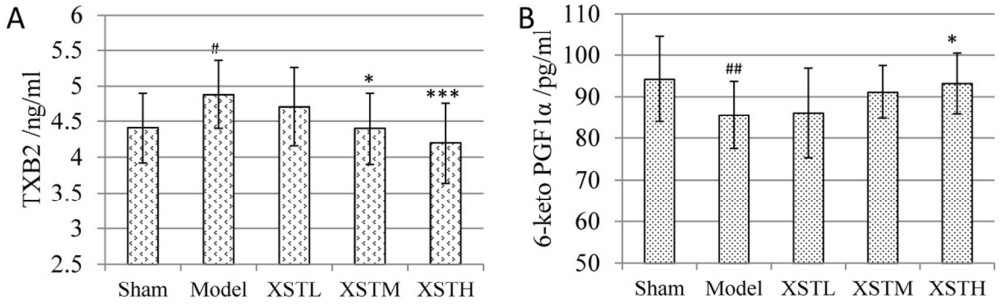

Figure 5. The effect of XST on NO production in RAW264.7 macrophages.

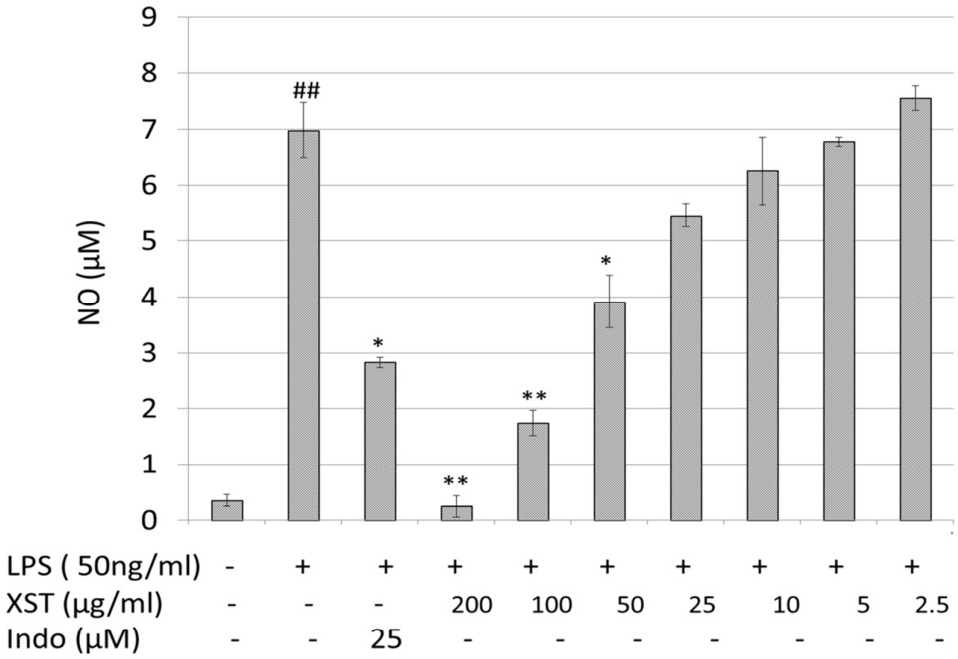

Tables

Table 1. Primer sequences used for the RT-PCR experiments

Gene	Forward primer (5'→3')	Reverse primer (5' →3')
Actb	ACATCCGTAAAGACCTCTATGCCAACA	GTGCTAGGAGCCAGGGCAGTAATCT
Fabp4	TGGAAACTCGTCTCCAGTGAGAA	CTGACCGGATGACGACCAAG
Plau	TTCTCACGAACAGTGCAAGCAG	CGGCCATCGATGTTACAGATAAG
Ltc4s	CTCTGGGTCGCCGGCATCTT	CTGCTGATTCGGAGGGCCTT
Igf1	GCACTCTGCTTGCTCACCTTTA	TCCGAATGCTGGAGCCATA
Hmox1	AGGTGCACATCCGTGCAGAG	CTTCCAGGGCCGTATAGATATGGTA
Spp1	GCCATGAGGACAAGCTAGTCC	AGGAACTGTGGTTTTGCCT
Timp1	CATCTCTGGCCTCTGGCATC	CATAACGCTGGTATAAGGTGGTCTC

Table 2. Top pathways of XST against stroke

Map title	Fisher P value	n of Genes
Complement and coagulation cascades	1.5E-06	11
Toll-like receptor signaling pathway	3.1E-04	10
Leukocyte transendothelial migration	1.1E-03	10
Intestinal immune network for IgA production	1.9E-03	6
Focal adhesion	6.8E-03	12
Cytokine-cytokine receptor interaction	0.0E+00	28
ECM-receptor interaction	6.5E-05	10
p53 signaling pathway	9.6E-03	6
MAPK signaling pathway	4.8E-03	15
Renin-angiotensin system	5.9E-05	5
Pathways in cancer	2.6E-03	18
Asthma	7.6E-03	4
Amyotrophic lateral sclerosis (ALS)	2.6E-03	6
Hypertrophic cardiomyopathy (HCM)	1.7E-03	8
Arachidonic acid metabolism	1.3E-04	8

Table 3. Top chemicals correlated with XST treatment in CMAP

cmap name	mean	n	enrichment	p	specificity	percent non-null
verteporfin	0.866	3	0.997	0	0	100
pronetalol	0.447	4	0.884	0	0	75
pivampicillin	0.249	4	0.865	0	0	50
sulfaphenazole	0.299	4	0.854	0.001	0	50
aminophylline	0.437	4	0.802	0.003	0.008	75
ouabain	0.296	4	0.767	0.006	0.096	50
caffeic acid	0.371	3	0.825	0.011	0.000	66
nifuroxazide	0.484	4	0.714	0.013	0.070	75
difenidol	0.456	3	0.792	0.018	0.038	66
6-bromoindirubi n-3'-oxime	0.381	7	0.540	0.018	0.082	57
nalbuphine	0.338	5	0.634	0.019	0.008	60
glafenine	0.317	4	0.672	0.026	0.057	50
piperlongumine	0.311	2	0.886	0.027	0.143	50
parthenolide	0.454	4	0.666	0.028	0.287	75
sulfathiazole	0.315	5	0.603	0.030	0.024	60
famotidine	0.227	5	0.600	0.031	0.008	60
epiandrosterone	0.275	4	0.636	0.043	0.084	50
papaverine	0.168	4	0.631	0.046	0.039	50

Table 4. The FCs of representative genes as determined by microarray and RT-PCR.

	FC1_microarray	FC2_microarray	FC1_RT-PCR	FC2_RT-PCR
Fabp4	156.82	2.59	261.57	1.76
Plau	33.90	2.26	41.47	1.25
Hmox1	10.50	1.91	8.04	1.33
Ltc4s	5.11	1.64	2.63	1.41
Igf1	22.74	1.81	12.68	1.24
Spp1	526.66	1.66	231.31	1.81